Mineralogical Magazine (2024), **88**, 40–48
doi:10.1180/mgm.2023.77

CAMBRIDGE UNIVERSITY PRESS

Article

Tellurium-rich stibiogoldfieldite and Se-bearing dantopaite from Goldfield, Nevada, USA: new crystal chemical data

Silvia Musetti[1], Jiří Sejkora[2], Cristian Biagioni[1,3] and Zdeněk Dolníček[2]

[1]Dipartimento di Scienze della Terra, Università di Pisa, Via Santa Maria 53, I-56126 Pisa, Italy; [2]Department of Mineralogy and Petrology, National Museum, Cirkusová 1740, 193 00, Praha 9, Czech Republic; and [3]CISUP, Centro per l'Integrazione della Strumentazione dell'Università di Pisa, Pisa, Italy

Abstract

Cotype material of stibiogoldfieldite from the Mohawk mine, Goldfield, Nevada, USA, has been examined in order to collect single-crystal X-ray diffraction data of Te-rich stibiogoldfieldite and to characterise the associated Ag–Bi–(S,Se) phase. Tellurium-rich stibiogoldfieldite, with empirical formula $(Cu_{11.30}Ag_{0.03})_{\Sigma 11.33}(Sb_{0.80}As_{0.57}Bi_{0.06}Te_{2.57})_{\Sigma 4.00}(S_{12.83}Se_{0.20})_{\Sigma 13.03}$, is cubic, space group $I\bar{4}3m$, with unit-cell parameters $a = 10.2947(3)$ Å and $V = 1091.04(10)$ Å^3. Its crystal structure has been refined to $R_1 = 0.0161$ for 397 unique reflections with $F_o > 4\sigma(F_o)$ and 25 refined parameters. The structure refinement confirmed the occurrence of a vacancy at the $M(2)$ site, in agreement with the substitution $^{M(2)}Cu^+ + {}^{X(3)}(Sb/As)^{3+} = {}^{M(2)}\square + {}^{X(3)}Te^{4+}$. The Ag–Bi–(S,Se) phase was identified as the ^6P homologue of the pavonite series, namely dantopaite. Its empirical formula is $Cu_{1.36}Ag_{4.39}Pb_{0.12}Bi_{12.62}Sb_{0.06}(S_{14.01}Se_{7.91}Te_{0.08})$, showing an exceptionally high Se content. Unit-cell parameters of Se-bearing dantopaite are $a = 13.518(2)$, $b = 4.0898(6)$, $c = 18.984(3)$ Å, $\beta = 106.816(6)°$, $V = 1004.7(3)$ Å^3 and space group $C2/m$. The crystal structure was refined to $R_1 = 0.0504$ for 1230 unique reflections with $F_o > 4\sigma(F_o)$ and 82 refined parameters. The metal excess (~0.55 atoms per formula unit) of this pavonite homologue is mainly due to the accumulation of Ag and Cu in the thin slab of the crystal structure, whereas the high Se content is related to the partial replacement of S occurring preferentially in the thick PbS-like slab. Domains richer in Se and Pb in dantopaite, with empirical formula $Cu_{0.89}Ag_{4.50}Pb_{0.49}Bi_{12.53}Sb_{0.07}(S_{11.26}Se_{10.74})$, were also identified, as grains up to 30 μm in size intimately intergrown with bohdanowiczite, indicating the possibility of a wide Se-to-S substitution in dantopaite.

Keywords: stibiogoldfieldite; tetrahedrite group; tellurium; dantopaite; pavonite homologous series; selenium; crystal structure; Mohawk mine; USA

(Received 8 August 2023; accepted 3 October 2023; Accepted Manuscript published online: 16 October 2023; Associate Editor: Owen Missen)

Introduction

Stibiogoldfieldite, ideally $Cu_{12}(Sb_2Te_2)S_{13}$, is a recently defined member of the tetrahedrite group, described from the Mohawk mine, Goldfield mining district, Nevada, USA (Biagioni *et al.*, 2022a). In the description of this new mineral, two specimens from the type locality were described. Holotype material has the chemical formula $(Cu_{12.05}Ag_{0.04}Zn_{0.03}Fe_{0.01})_{\Sigma 12.13}(Sb_{1.12}As_{0.63}Bi_{0.23}Te_{2.02})_{\Sigma 4.00}(S_{12.99}Se_{0.11})_{\Sigma 13.10}$, whereas cotype material is richer in Te, with empirical chemical formula $(Cu_{11.30}Ag_{0.03})_{\Sigma 11.33}(Sb_{0.80}As_{0.57}Bi_{0.06}Te_{2.57})_{\Sigma 4.00}(S_{12.83}Se_{0.20})_{\Sigma 13.03}$, close to the idealised formula $(Cu_{11.40}\square_{0.60})_{\Sigma 12.00}(Sb_{0.80}As_{0.55}Bi_{0.05}Te_{2.60})_{\Sigma 4.00}(S_{12.80}Se_{0.20})_{\Sigma 13.00}$. The higher Te content of this latter sample was coupled with a (Cu+Ag) deficit, in agreement with the substitution $^{M(2)}Cu^+ + {}^{X(3)}(Sb/As)^{3+} = {}^{M(2)}\square + {}^{X(3)}Te^{4+}$ (e.g. Shimizu and Stanley, 1991; Biagioni *et al.*, 2022a). The occurrence of vacancies at the $M(2)$ site in the crystal structure of synthetic Te-bearing tetrahedrites was first proposed by Kalbskopf (1974) and later confirmed on natural specimens by Dmitrieva *et al.* (1987), using single-crystal X-ray diffraction data collected on arsenogoldfieldite, and by Pohl *et al.* (1996), on the basis of Rietveld refinement performed on samples with composition $Cu_{11.1}(Te_{2.7}Sb_{0.9}As_{0.4}Bi_{0.1})S_{12.0}Se_{0.7}$. The resulting formula of the Te end-member goldfieldite is thus $Cu_{10}Te_4S_{13}$, also agreeing with the theoretical model based on a Brillouin-model analysis (Johnson and Jeanloz, 1983).

Holotype material of stibiogoldfieldite has been fully characterised, both chemically and structurally; however the cotype material has only been studied chemically (Biagioni *et al.*, 2022a). In order to fill this gap, a single-crystal X-ray diffraction study was performed on the Te-rich stibiogoldfieldite. Moreover, an associated and still unidentified Ag–Bi–(S,Se) phase was investigated. This latter species was observed in both holotype and cotype material of stibiogoldfieldite (Biagioni *et al.*, 2022a) and chemical data indicated it could belong to the pavonite homologous series (unpublished data). The single-crystal X-ray diffraction results (below) confirm this hypothesis, allowing its identification as the $N = 6$ homologue of the pavonite series, namely dantopaite. Further, this sample showed a peculiar chemical composition, being Se-enriched, hence its crystal structure

Corresponding author: Cristian Biagioni; Email: cristian.biagioni@unipi.it
Cite this article: Musetti S., Sejkora J., Biagioni C. and Dolníček Z. (2024) Tellurium-rich stibiogoldfieldite and Se-bearing dantopaite from Goldfield, Nevada, USA: new crystal chemical data. *Mineralogical Magazine* **88**, 40–48. https://doi.org/10.1180/mgm.2023.77

was refined, in order to understand the behaviour of Se in this compound.

This study has consequently a two-fold aim: an improvement of the crystal chemical knowledge of Te-bearing tetrahedrites and the crystal-chemical study of Se-bearing dantopaite associated with stibiogoldfieldite at the Mohawk mine.

Experimental

Specimen studied

The specimen studied is represented by cotype material of stibiogoldfieldite, kept in the mineralogical collection of the Department of Mineralogy and Petrology of the National Museum in Prague (Czech Republic), under catalogue number P1P 80/2020. Stibiogoldfieldite forms anhedral grains, up to 0.3 mm, associated with pyrite, calaverite, bismuthinite, bohdanowiczite and Se-bearing dantopaite (Fig. 1).

Chemical analysis

Quantitative chemical analysis of stibiogoldfieldite and Se-bearing dantopaite were performed using a Cameca SX 100 electron microprobe (National Museum of Prague, Czech Republic) and the following analytical conditions: wavelength dispersive spectroscopy mode, accelerating voltage of 25 kV, beam current of 20 nA and beam diameter of 0.7 μm. Standards (element, emission line) were: chalcopyrite (Cu$K\alpha$, S$K\alpha$); Ag metal (Ag$L\alpha$); Sb_2S_3 (Sb$L\alpha$); PbTe (Te$L\alpha$); PbS (Pb$M\alpha$); Bi_2Se_3 (Bi$M\beta$); and PbSe (Se$L\beta$). Contents of other elements with $Z > 8$ are below detection limits. Matrix correction by PAP software (Pouchou and Pichoir, 1985) was applied to the data. Electron microprobe data of Te-rich stibiogoldfieldite were given in Biagioni *et al.* (2022a), whereas the results on Se-bearing dantopaite are reported in Tables 1 and 2.

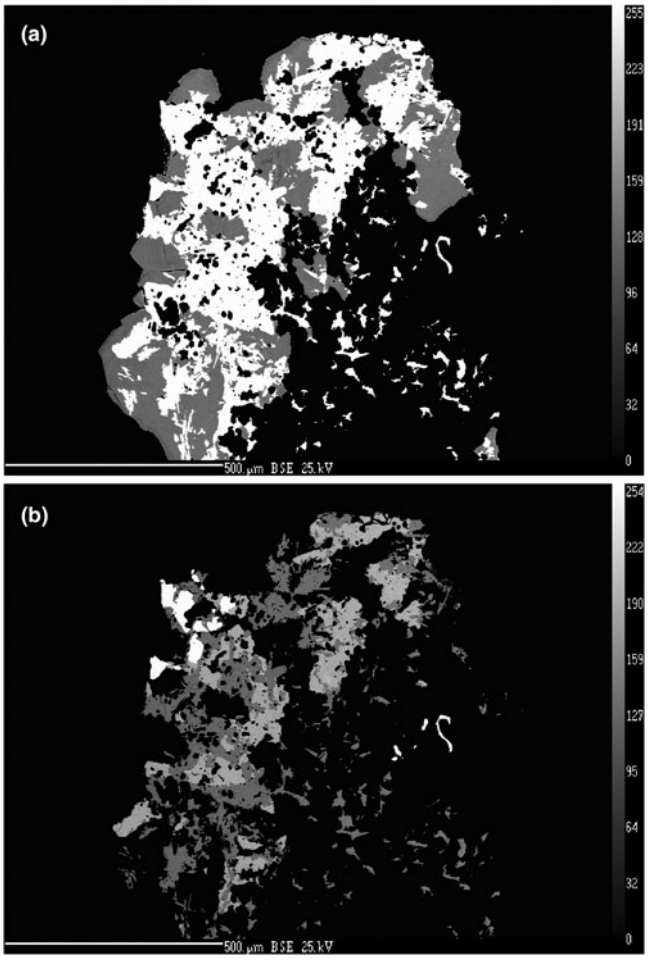

Figure 1. Back-scattered electron image of the cotype specimen of stibiogoldfieldite. Two different degrees of contrast and brightness have been applied in (a) and (b), in order to show all the mineral species. In (a), Te-rich stibiogoldfieldite is grey, whereas all the other phases are white; in (b), Se-bearing dantopaite is dark grey, calaverite is grey, and gold is white. Cotype specimen, National Museum of Prague (Czech Republic), catalogue number P1P 80/2020.

Single-crystal X-ray diffraction

Single-crystal X-ray diffraction intensity data of cotype stibiogoldfieldite and Se-bearing dantopaite were collected using a Bruker D8 Venture diffractometer (50 kV and 1.4 mA) equipped with an air-cooled Photon III detector, and microfocus Mo$K\alpha$ radiation (C.I.S.U.P., University of Pisa, Italy). The detector-to-crystal distance was set to 38 mm. For both data collections, frames were integrated with the Bruker *SAINT* software package using a narrow-frame algorithm. Data were then corrected for Lorentz-polarisation, absorption and background. Neutral scattering curves were taken from the *International Tables for Crystallography* (Wilson, 1992).

Intensity data of stibiogoldfieldite were collected using φ and ω scan modes, in 0.5° slices, with an exposure time of 10 s per frame. A total of 632 frames was collected. Unit-cell parameters, refined on the basis of the XYZ centroids of 4891 reflections above 20 σI with $5.596 < 2\theta < 64.959°$, are $a = 10.2947(3)$ Å, $V = 1091.04(10)$ Å^3 and space group $I\bar{4}3m$. The crystal structure of cotype stibiogoldfieldite was refined using *Shelxl*-2018 (Sheldrick, 2015) starting from the atomic coordinates of stibiogoldfieldite (Biagioni *et al.*, 2022a). The following neutral scattering curves were used: Cu *vs* □ at the $M(2)$ and $M(1)$ sites, Te *vs* As at $X(3)$, and S at S(1) and S(2) sites. The $M(2)$ site was found to be split and the site occupancy at both sub-positions were refined independently. After several cycles of anisotropic refinement, the agreement factor R_1 converged to 0.0161 for 397 unique reflections with $F_o > 4\sigma(F_o)$ and 25 refined parameters. An unsplit model was also refined in order to compare the current results with those given in Biagioni *et al.* (2022a).

Intensity data of Se-bearing dantopaite were collected in φ and ω scan modes, in 0.5° slices, with an exposure time of 10 s per frame. A total of 1272 frames was collected. Unit-cell parameters, refined on the basis of the XYZ centroids of 3057 reflections above 20 σI with

Table 1. Chemical data for Se-bearing dantopaite.

Element	wt.%	Range (n = 80)	e.s.d.	apfu	Range	e.s.d.
Cu	2.01	1.43–2.61	0.28	1.36	0.98–1.75	0.19
Ag	10.99	10.39–11.56	0.27	4.39	4.16–4.70	0.11
Pb	0.56	0.37–0.77	0.09	0.12	0.08–0.16	0.02
Sb	0.17	0.09–0.24	0.03	0.06	0.03–0.08	0.01
Bi	61.19	59.06–62.52	0.76	12.62	12.33–12.89	0.13
S	10.42	9.13–11.65	0.48	14.01	12.72–15.36	0.53
Se	14.49	12.28–17.17	0.87	7.91	6.58–9.49	0.53
Te	0.23	0.16–0.34	0.04	0.08	0.05–0.12	0.01
Total	100.05	98.27–101.50	0.48			

e.s.d. = estimated standard deviation; apfu = atoms per formula unit.

https://doi.org/10.1180/mgm.2023.77 Published online by Cambridge University Press

Table 2. Chemical data for Se-bearing, Pb-enriched, dantopaite.

Element	wt.%	Range (n = 31)	e.s.d.	apfu	Range	e.s.d.
Cu	1.25	0.97–1.53	0.14	0.89	0.70–1.09	0.09
Ag	10.73	10.41–11.21	0.19	4.50	4.35–4.78	0.10
Pb	2.23	2.05–2.46	0.10	0.49	0.45–0.55	0.03
Sb	0.20	0.15–0.24	0.02	0.07	0.06–0.09	0.01
Bi	57.97	56.94–59.19	0.71	12.53	12.35–12.72	0.11
S	7.99	7.72–8.23	0.14	11.26	11.08–11.46	0.13
Se	18.77	18.22–19.33	0.25	10.74	10.54–10.92	0.13
Te	0.00					
Total	99.14	98.02–100.29	0.48			

e.s.d. = estimated standard deviation; apfu = atoms per formula unit.

$6.042 < 2\theta < 56.50°$, are $a = 13.518(2)$, $b = 4.0898(6)$, $c = 18.984(3)$ Å, $\beta = 106.816(6)°$, $V = 1004.7(3)$ Å^3 and space group $C2/m$. The crystal structure of this phase was solved initially through direct methods using *Shelxt* and was refined using *Shelxl*-2018 (Sheldrick, 2015). Once it was clear that this phase corresponded to the $N = 6$ homologue of the pavonite homologous series, the atomic coordinates were recast into those given by Makovicky *et al.* (2010) for dantopaite. The following neutral scattering curves were used: Bi *vs* Ag at the $M(1)$–$M(4)$ [$M(4)$ was found fully occupied by Bi] and S *vs* Se at S(1)–S(6) sites. The site occupancies at the *Ag*, *Cu*(1), and *Cu*(2) sites were refined freely using the scattering curves of Ag and Cu. After several cycles of anisotropic refinement, the agreement factor R_1 converged to 0.0504 for 1230 unique reflections with $F_o > 4\sigma(F_o)$ and 82 refined parameters.

Data collection details and refinements for both stibiogoldfieldite and dantopaite are in Table 3, whereas fractional atomic coordinates and displacement parameters, as well as selected bond distances, are given in Tables 4 and 5. Bond-valence sums (BVS), calculated using the bond parameters of Brese and O'Keeffe (1991) are in Tables 6 and 7. The crystallographic information files (cifs) have been deposited with the Principal Editor of *Mineralogical Magazine* and are available as Supplementary material (see below).

Results and discussion

Tellurium-rich stibiogoldfieldite

The crystal structure of cotype stibiogoldfieldite agrees with the general features of the members of the tetrahedrite group. As reported in the Introduction, previous chemical data given by Biagioni *et al.* (2022a) indicated that cotype stibiogoldfieldite is Te-rich, with 2.57 Te atoms per formula unit (apfu). Such a Te content should be coupled with the occurrence of vacancy (□) at the $M(2)$ site and the composition of cotype material should be idealised as $(Cu_{11.4}\square_{0.6})[(Sb_{0.8}As_{0.6})_{\Sigma 1.4}Te_{2.6}]S_{13} = {}^{M(2)}(Cu_{5.4}\square_{0.6})^{M(1)}Cu_6{}^{X(3)}[Sb_{0.8}As_{0.6}Te_{2.6}]^{S(1)}S_{12}{}^{S(2)}S$.

In the material studied, the $M(2)$ site is split into two sub-positions $M(2a)$ and $M(2b)$, with $M(2a)$–$M(2b) = 0.52(4)$ Å. The first one shows a planar triangular coordination, whereas the second one has a flat trigonal pyramidal coordination, in agreement with previous studies (e.g. Welch *et al.*, 2018; Sejkora *et al.*, 2021; Biagioni *et al.*, 2022b). Average Me–S bond distances are 2.219 and 2.288 Å for $M(2a)$ and $M(2b)$, respectively. Both sub-positions are partially occupied by Cu, whereas the Ag content is negligible (≈0.03 apfu, according to electron microprobe analysis). In holotype stibiogoldfieldite, the $M(2)$ site was not found split. In order to compare the Me–S bond distances observed in holotype and cotype specimens, an unsplit model of cotype material was refined ($R_1 = 0.0194$). The average Me–S bond distance at $M(2)$ is 2.230 Å, to be compared with 2.251 Å observed by Biagioni *et al.* (2022a) in the holotype sample. The observed mean atomic number (MAN) at $M(2a) + M(2b)$ corresponds to 25.64 electrons, comparable to those calculated from electron microprobe analysis, i.e. 25.84 electrons assuming the site occupancy ${}^{M(2)}(Cu_{0.883}Ag_{0.005}\square_{0.112})$, thus supporting the occurrence of a vacancy at the $M(2)$ site. In holotype material, $M(2)$ was found fully occupied by Cu. The bond-valence sum for $M(2a) + M(2b)$ is 0.97 valence units (vu), in accord with the presence of monovalent Cu.

The tetrahedrally coordinated $M(1)$ site is a pure Cu site. The average Me–S bond distance is 2.323 Å, close to the $<M(1)$–S(1)$>$ distance of 2.329 Å observed in holotype material (Biagioni *et al.*, 2022a). The observed MAN, 28.56 electrons, agrees with the theoretical value of 29.00 electrons. The BVS at $M(1)$ is 1.16 vu.

The $X(3)$ site, on the basis of electron microprobe data, should have the site occupancy $(Te_{0.64}Sb_{0.20}As_{0.14}Bi_{0.02})$ which corresponds to a calculated MAN of 49.76 electrons, in accord with the value obtained during the crystal structure refinement, i.e. 48.96 electrons. In holotype stibiogoldfieldite, the site occupancy at the $X(3)$ site is $(Te_{0.50}Sb_{0.28}As_{0.16}Bi_{0.06})$ (Biagioni *et al.*, 2022a). The higher amount of Te and the lower content of Sb in cotype material results in a slight contraction of the average

Table 3. Summary of crystal data and parameters describing data collections and refinements for Te-rich stibiogoldfieldite and Se-bearing dantopaite.

	Te-rich stibiogoldfieldite	Se-bearing dantopaite
Crystal data		
Crystal size (mm)	0.100×0.090×0.075	0.080×0.075×0.050
Space group	$I\bar{4}3m$	$C2/m$
a (Å)	10.2947(3)	13.518(2)
b (Å)	-	4.0898(6)
c (Å)	-	18.984(3)
β (°)	-	106.816(6)
V (Å^3)	1091.04(10)	1004.7(3)
Z	2	1
Data collection		
Radiation, wavelength (Å)	Mo$K\alpha$, λ = 0.71073	Mo$K\alpha$, λ = 0.71073
Temperature (K)	293(2)	293(2)
$2\theta_{max}$ (°)	64.96	56.69
Measured reflections	5177	6840
Unique reflections	397	1419
Reflections with $F_o > 4\sigma(F_o)$	393	1230
R_{int}	0.0357	0.0607
$R\sigma$	0.0181	0.0466
Range of h, k, l	$-13 \le h \le 15$, $-14 \le k \le 15$, $-15 \le l \le 15$	$-17 \le h \le 17$, $-5 \le k \le 5$, $-24 \le l \le 25$
Refinement		
R_1 [$F_o > 4\sigma(F_o)$]	0.0161	0.0504
R_1 (all data)	0.0162	0.0586
wR_2 (on F_o^2)[1]	0.0434	0.1156
Goof	1.106	1.050
Absolute structure parameter [2]	0.05(4)	-
Number of least-squares parameters	25	82
Maximum and minimum residual peak (e Å^{-3})	+0.63 [at 0.67 Å from $X(3)$] −0.55 [at 0.71 Å from $X(3)$]	+3.04 [at 0.77 Å from $M(3)$] −2.74 [at 1.04 Å from Se(4)]

[1] $w = 1/[\sigma^2(F_o^2) + (0.0271P)^2 + 1.6352P]$ for Te-rich stibiogoldfieldite; $w = 1/[\sigma^2(F_o^2) + (0.0001P)^2 + 265.7769\ P]$ for Se-bearing dantopaite.
[2] Flack (1983)

https://doi.org/10.1180/mgm.2023.77 Published online by Cambridge University Press

Table 4. Sites, Wyckoff positions, site occupancy, fractional atomic coordinates and isotropic (*) or equivalent isotropic displacement parameters (Å^2) for Te-rich stibiogoldfieldite and Se-bearing dantopaite.

Site	Wyckoff position	Site occupancy	*x/a*	*y/b*	*z/c*	U_{eq}
Te-rich stibiogoldfieldite						
M(2a)	12e	$Cu_{0.73(3)}$	0.7857(2)	0	0	0.0318(18)
M(2b)	24g	$Cu_{0.077(15)}$	0.7829(12)	0.036(2)	–0.036(2)	0.0318(18)
M(1)	12d	$Cu_{0.985(10)}$	¾	½	0	0.0249(4)
X(3)	8c	$Te_{0.84(2)}As_{0.16(2)}$	0.73833(3)	0.73833(3)	0.73833(3)	0.01550(17)
S(1)	24g	$S_{1.00}$	0.88590(9)	0.88590(9)	0.63941(11)	0.0162(4)
S(2)	2a	$S_{1.00}$	0	0	0	0.0239(8)
Se-bearing dantopaite						
M(1)	4*i*	$Bi_{0.667(14)}Ag_{0.333(14)}$	0.85712(9)	0	0.34828(6)	0.0216(4)
M(2a)	4*i*	$Bi_{0.699(15)}$	0.6154(8)	0	0.4485(5)	0.0238(8)
M(2b)	4*i*	$Ag_{0.301(15)}$	0.621(4)	0	0.441(2)	0.0238(8)
M(3)	4*i*	$Bi_{0.832(15)}Ag_{0.167(15)}$	0.09935(8)	0	0.24890(5)	0.0198(4)
M(4)	4*i*	$Bi_{1.00}$	0.31243(8)	0	0.09881(5)	0.0241(3)
Ag	2*a*	$Ag_{0.66(2)}$	0	0	0	0.076(3)
Cu(1)	4*i*	$Cu_{0.10(2)}$	0.515(4)	0	0.046(3)	0.06(2)*
Cu(2)	4*g*	$Cu_{0.21(2)}$	0	0.292(9)	0	0.065(12)*
S(1)	4*i*	$S_{0.91(2)}Se_{0.09(2)}$	0.6633(4)	0	0.0333(3)	0.0155(16)
S(2)	4*i*	$S_{0.54(3)}Se_{0.46(3)}$	0.2472(3)	0	0.4102(3)	0.0354(17)
S(3)	4*i*	$Se_{0.57(2)}S_{0.43(2)}$	0.7236(3)	0	0.21584(17)	0.0207(11)
S(4)	2*c*	$Se_{0.66(4)}S_{0.34(4)}$	0	0	½	0.074(4)
S(5)	4*i*	$Se_{0.55(2)}S_{0.45(2)}$	0.4799(3)	0	0.3046(2)	0.0241(12)
S(6)	4*i*	$S_{0.82(2)}Se_{0.18(2)}$	0.9660(4)	0	0.1160(3)	0.0296(19)

<*X*(3)–S(1)> distance. Indeed, this value is 2.387(4) Å in the holotype specimen, and 2.3775(12) Å in cotype material. This is in keeping with the shorter Te–S distances with respect to Sb–S ones. The bond-valence sum at the *X*(3) site is 3.48 vu, to be compared with the theoretical value of 3.64 vu based on the *X*(3) site occupancy.

Table 5. Selected bond distances (in Å) for Te-rich stibiogoldfieldite and Se-bearing dantopaite.

Te-rich stibiogoldfieldite			
M(1)–S(1)×4	2.3231(7)	*M*(2b)–S(1)×2	2.283(9)
		M(2b)–S(2)	2.295(17)
		Average	2.287
M(2a)–S(2)	2.206(2)	*X*(3)–S(1)×3	2.3775(12)
M(2a)–S(1)×2	2.2420(17)		
Average	2.230		
Se-bearing dantopaite			
M(1)–S(3)	2.637(3)	*M*(2a)–S(2)	2.786(12)
M(1)–S(5)	2.901(3)×2	*M*(2a)–S(5)	2.815(11)
M(1)–S(2)	2.964(3)×2	*M*(2a)–S(4)	2.907(5)×2
M(1)–S(4)	2.9677(11)	*M*(2a)–S(2)	2.938(6)×2
Average	2.889	Average	2.882
M(2b)–S(5)	2.74(5)	*M*(3)–S(6)	2.643(5)
M(2b)–S(2)	2.83(3)×2	*M*(3)–S(3)	2.829(2)×2
M(2b)–S(2)	2.87(5)	*M*(3)–S(5)	2.983(3)×2
M(2b)–S(4)	3.02(3)×2	*M*(3)–S(2)	3.135(5)
Average	2.88	Average	2.900
M(4)–S(1)	2.622(5)	*Ag*–S(6)	2.376(6)×2
M(4)–S(6)	2.864(4)×2	*Ag*–S(1)	2.940(4)×4
M(4)–S(1)	2.888(3)×2	Average	2.752
Average	2.825		
M(4)–S(3)	3.479(3)×2		
Cu(1)–S(1)	2.09(5)	*Cu*(2)–S(1)	2.275(14)×2
Cu(1)–S(1)	2.45(5)	*Cu*(2)–S(6)	2.662(16)×2
Cu(1)–S(6)	2.62(4)×2		

The S(1) site is four-fold coordinated and is bonded to two *M*(1), one *M*(2) and one *X*(3). Its BVS is 2.06 vu. S(2) is octahedrally coordinated by atoms hosted at *M*(2) sites, with BVS of 1.98 vu. Both sites are fully occupied by S. Minor Se (0.20 apfu, as detected by electron microprobe analysis) was located at neither of the S(1) or S(2) sites; it could possibly be disordered among the two positions.

Se-bearing dantopaite

Dantopaite, ideally $Ag_5Bi_{13}S_{22}$, is the ^6P homologue of the pavonite series (Makovicky *et al.*, 2010). In addition to its type locality, Erzwies, Austria, it is currently reported only from the Rozália mine, Slovakia and the Clara mine, Germany (Jeleň *et al.*, 2012; Kolitsch *et al.*, 2019). The identification of dantopaite at the Mohawk mine, Goldfield, USA, is thus the fourth world-occurrence.

Chemical composition

The chemical formula of dantopaite from the Mohawk mine (Table 1), calculated on the basis of 22 (S+Se+Te) apfu, is $Cu_{1.36}Ag_{4.39}Pb_{0.12}Bi_{12.62}Sb_{0.06}(S_{14.01}Se_{7.91}Te_{0.08})$. The empirical formula shows an excess of cations (~0.55 apfu), probably as a result of the accumulation of Cu in the column of octahedra in the thinner slab, in agreement with the structural model of

Table 6. Weighted bond-valence sums (in valence units) for Te-rich stibiogoldfieldite.

Site	*M*(1)	*M*(2a)	*M*(2b)	*X*(3)	Σanions	Theor.
S(1)	$^{2\times\rightarrow}0.29^{\times4\downarrow}$	$0.26^{\times2\downarrow}$	$^{2\times\rightarrow}0.03^{\times2\downarrow}$	$1.16^{\times3\downarrow}$	2.06	2.00
S(2)		$^{6\times\rightarrow}0.29$	$^{12\times\rightarrow}0.02$		1.98	2.00
Σcations	1.16	0.81	0.08	3.48		
Theor.	1.00	0.73	0.08	3.64		

Note: left and right superscripts indicate the number of equivalent bonds involving cations and anions, respectively. The following site occupancies were used: *M*(2a) = $Cu_{0.73}$; *M*(2b) = $Cu_{0.08}$; *M*(1) = $Cu_{1.00}$; *X*(3) = $Te_{0.64}Sb_{0.20}As_{0.14}Bi_{0.02}$.

https://doi.org/10.1180/mgm.2023.77 Published online by Cambridge University Press

Table 7. Weighted bond-valence sums (in valence units) for Se-bearing dantopaite.

Site	*M*(1)	*M*(2a)	*M*(2b)	*M*(3)	*M*(4)	*Ag*	*Cu*(1)	*Cu*(2)	Σanions	Theor.
S(1)					0.87	$^{2\times\rightarrow}0.08^{\times4\downarrow}$	0.06	$^{2\times\rightarrow}0.07^{\times2\downarrow}$	2.09	2.00
					$^{2\times\rightarrow}0.42^{\times2\downarrow}$		0.02			
S(2)	$^{2\times\rightarrow}0.32^{\times2\downarrow}$	0.47	$^{2\times\rightarrow}0.06^{\times2\downarrow}$	0.23					2.13	2.00
		$^{2\times\rightarrow}0.31^{\times2\downarrow}$	0.05							
S(3)	0.81			$^{2\times\rightarrow}0.55^{\times2\downarrow}$	$^{2\times\rightarrow}0.11^{\times2\downarrow}$				2.13	2.00
S(4)	$^{2\times\rightarrow}0.34$	$^{4\times\rightarrow}0.37^{\times2\downarrow}$	$^{4\times\rightarrow}0.04^{\times2\downarrow}$						2.32	2.00
S(5)	$^{2\times\rightarrow}0.39^{\times2\downarrow}$	0.45	0.07	$^{2\times\rightarrow}0.36^{\times2\downarrow}$					2.02	2.00
S(6)				0.76	$^{2\times\rightarrow}0.47^{\times2\downarrow}$	$0.38^{\times2\downarrow}$	$^{2\times\rightarrow}0.01^{\times2\downarrow}$	$^{2\times\rightarrow}0.03^{\times2\downarrow}$	2.16	2.00
Σcations	2.57	2.28	0.32	2.81	2.87	1.08	0.10	0.20		
Theor.	2.33	2.10	0.30	2.66	3.00	0.66	0.10	0.21		

Note: left and right superscripts indicate the number of equivalent bonds involving cations and anions, respectively. The site occupancies given in Table 4 for both cations and anions were used.

Makovicky *et al.* (2010). In addition to this predominant mineral, which was used for the crystal structure study, rare grains with higher Pb and Se contents (Fig. 2a), up to 30 μm in size, were also found in the polished sections (Table 2). Their average chemical formula, calculated on the same basis, is $Cu_{0.89}Ag_{4.50}Pb_{0.49}Bi_{12.53}Sb_{0.07}(S_{11.26}Se_{10.74})$ and shows an excess

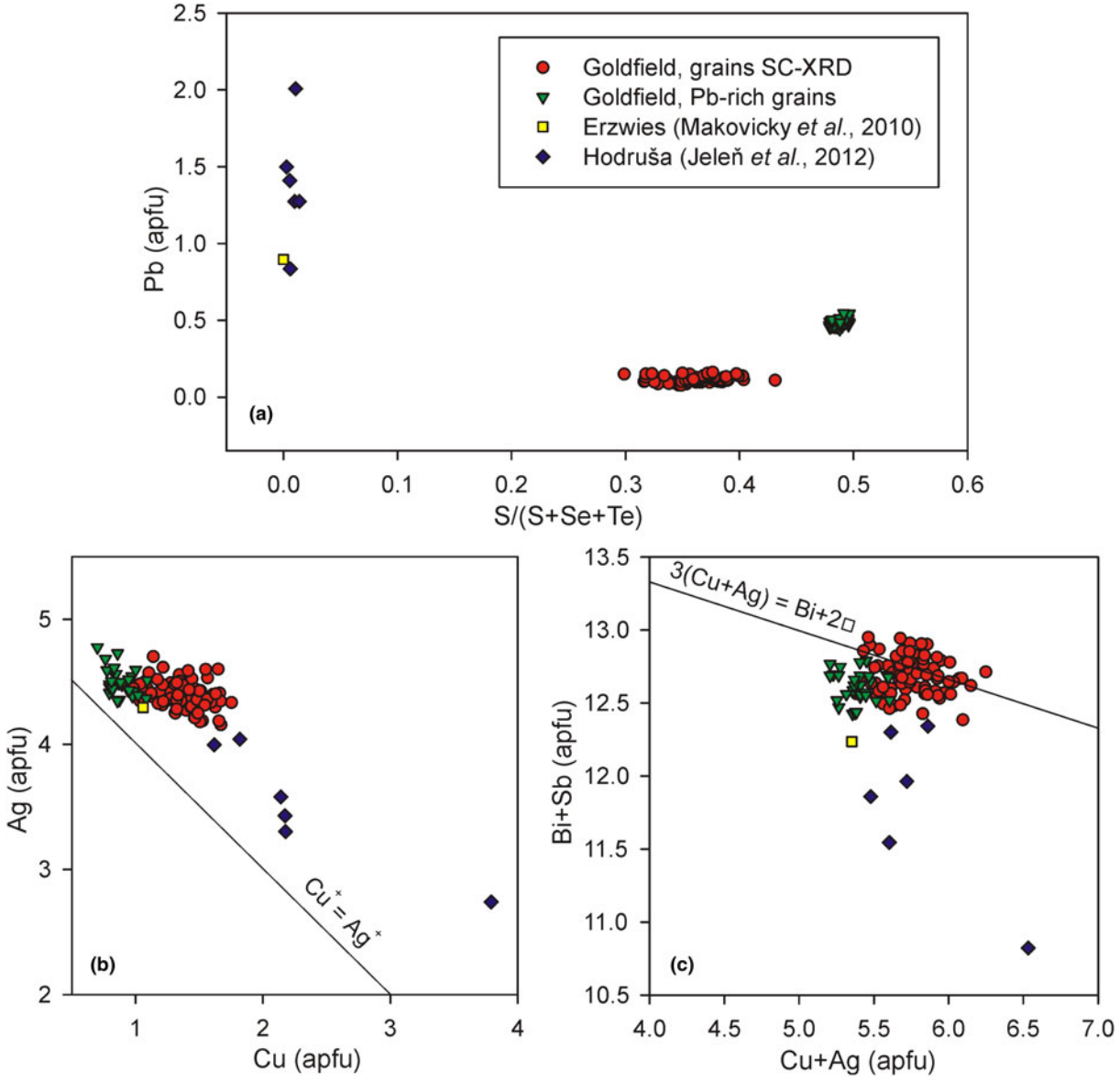

Figure 2. Relationship between (a) S/(S+Se+Te) and Pb; (b) Cu and Ag; and (c) (Cu+Ag) and (Bi+Sb), in atoms per formula unit (apfu), in Se-bearing dantopaite. Lines indicate the theoretical trend of the corresponding substitutions. For comparison, literature data are shown from Makovicky *et al.* (2010) and Jeleň *et al.* (2012).

https://doi.org/10.1180/mgm.2023.77 Published online by Cambridge University Press

of cations corresponding to ~0.48 apfu. These grains are usually intergrown with S-bearing bohdanowiczite ($Ag_{1.01}Bi_{1.01}Se_{1.37}S_{0.61}$).

Karup-Møller and Makovicky (1979) distinguished two different kinds of Cu, on the basis of their structural role. They identified some Cu fitting the ideal formula of pavonite homologues which they indicated as "substitutional Cu", ^{s}Cu, and some Cu occurring in the interstices of the crystal structure, namely "interstitial Cu", ^{i}Cu. On the basis of this distinction, they proposed three possible N numbers (N = order number of the homologue within the pavonite series) assuming that all Cu is interstitial (N_{P1}), all Cu is substitutional (N_{P2}), and that Cu is equally distributed between ^{s}Cu and ^{i}Cu (N_{P3}). These three different approaches led to the following values (minor Sb was added to Bi): $N_{P1} = 5.29$; $N_{P2} = 5.95$; and $N_{P3} = 5.62$ for the variety studied through single-crystal X-ray diffraction and $N_{P1} = 5.69$; $N_{P2} = 6.13$; and $N_{P3} = 5.91$ for the Se- and Pb-enriched grains. These values may suggest that Cu acts both as a substitutional and interstitial cation in the material studied.

Dantopaite from the Mohawk mine has some chemical peculiarities with respect to previous known occurrences.

(1) The Cu content is similar with that measured in dantopaite from the type locality, with a Cu/(Cu+Ag) atomic ratio of 0.24 (0.16 in the case of Pb-enriched variety), to be compared with 0.20 measured by Makovicky *et al.* (2010). In dantopaite from the Rozália mine, Cu/(Cu+Ag) = 0.38 (Jeleň *et al.*, 2012), indicating a larger replacement of Ag by Cu.

(2) The Pb content in dantopaite from the Mohawk mine is the lowest so far reported for the species. Indeed, only 0.12 Pb apfu were measured (0.49 for Pb-enriched variety), to be compared with 0.90 and 1.32 apfu in dantopaite from Erzwies and the Rozália mine, respectively (Makovicky *et al.*, 2010; Jeleň *et al.*, 2012).

(3) Bismuth is replaced by minor Sb (0.06–0.07 apfu).

(4) The metal excess is 0.55 apfu (0.48 apfu for the Pb-enriched variety), to be compared with 0.43 apfu in dantopaite from the Austrian type locality (Makovicky *et al.*, 2010); this excess is definitely lower than that found in the sample from Slovakia, i.e. 1.43 apfu (Jeleň *et al.*, 2012).

(5) The Se content is exceptional, with a Se/(S+Se+Te) ratio of 0.360 for sample used for single crystal study and even 0.488 in the case of Pb-enriched variety. In type dantopaite, S was replaced by minor Te (0.11 apfu, similar to that detected in the sample from the Mohawk mine), but no Se was reported. On the contrary, Jeleň *et al.* (2012) gave 0.15 Se apfu, i.e. Se/(S+Se+Te) = 0.007.

In the empirical formula of dantopaite from the Mohawk mine, several homo- and heterovalent substitutions take place. A 'substitution-free' formula of dantopaite used for the structural study can be obtained applying the following substitutions. Selenium and minor Te can be accounted for through the substitution $(Se,Te)^{2-} = S^{2-}$ (Fig. 2a) and minor Sb^{3+} is replaced by Bi^{3+} according to the homovalent substitution $Sb^{3+} = Bi^{3+}$. The occurrence of Pb could be related to the substitution $Cu^{+} + Pb^{2+} = \square + Bi^{3+}$; after subtracting minor Pb, the formula is $Cu_{1.24}Ag_{4.39}Bi_{12.80}S_{22}$. The presence of Cu can be partially due to the $Ag^{+} = Cu^{+}$ substitution, however, Fig. 2b does not show a clear negative relationship between these two elements and their mutual replacement does not explain the remaining metal excess, i.e. 0.43 apfu. A possible mechanism could involve the replacement of Bi^{3+} by Cu^{+} (or Ag^{+}) and the occupancy of interstitial positions by Cu^{+}, according to the substitution rule $3(Cu, Ag)^{+} = Bi^{3+} + 2\square$ (Fig. 2c). In this equation, one could consider the amount of Bi^{3+} as the difference between its ideal content (13 apfu) and 12.80 apfu, i.e. 0.20. Using this calculation the formula can be recast as $Cu_{0.64}Ag_{4.39}Bi_{13.00}S_{22}$. However, alternatively, one could assume that $2\square = 0.43$ apfu, and then the formula becomes $Cu_{0.595}Ag_{4.39}Bi_{13.015}S_{22}$. The homovalent substitution $Cu^{+} = Ag^{+}$ leads to $Ag_{5.03}Bi_{13.00}S_{22}$ and $Ag_{4.985}Bi_{13.015}S_{22}$, respectively, close to the ideal formula $Ag_5Bi_{13}S_{22}$.

Crystal structure

The crystal structure of Se-bearing dantopaite is isotypic with that of dantopaite (Makovicky *et al.*, 2010) and it is composed of two kinds of slabs parallel to (001), i.e. a PbS-like thick slab and a thin slab (Fig. 3).

The thicker slab is formed by Bi- and Ag-centred octahedra, namely the $M(1)$–$M(3)$ sites. In agreement with the order number $N = 6$, there are six octahedra in a diagonal row across the thicker slab, according to the sequence $M(3)$–$M(1)$–$M(2)$–$M(2)$–$M(1)$–$M(3)$.

The $M(1)$ site is a mixed (Bi,Ag) position, with a Bi/(Bi+Ag) ratio of 0.66. In type dantopaite, this site has a pure Bi occupancy. The site is characterised by a short $M(1)$–S(3) bond of 2.637 Å, with S(3) located on interslab surfaces. This distance is shorter than that observed in dantopaite from Erzwies (2.664 Å), notwithstanding the significant replacement of S by Se [site occupancy at $S(3) = Se_{0.57}S_{0.43}$]. The coordination of $M(1)$ is completed by five additional bonds ranging between 2.901 and 2.968 Å. The average <$M(1)$–S> distance is 2.889 Å, longer than that observed in dantopaite (2.832 Å) and agreeing with the replacement of S by the larger anion Se^{2-}. The bond-valence sum at this site is 2.57 vu, slightly higher than the theoretical value of 2.33 vu based on the proposed site occupancy.

The $M(2)$ site is located at the centre of the thick PbS-like slab. In agreement with Makovicky *et al.* (2010), this position is actually split into two sub-positions, occupied by Bi [$M(2a)$] and Ag [$M(2b)$], respectively, with a Bi/(Bi+Ag) ratio of 0.70. In the sample studied by Makovicky *et al.* (2010), the $M(2)$ site hosted Pb and was split into two sub-positions, with a ratio 82:18. Both sub-positions have the same average distance (~2.88 Å, slightly longer than those observed in dantopaite from Erzwies, i.e. ~2.85 Å), with $M(2a)$ more regular than $M(2b)$. A more pronounced distortion was observed in the Austrian sample, with bond distances at the *Ag2* position ranging between 2.59 and 3.03 Å; in dantopaite from the Mohawk mine such distances range between 2.74 and 3.03 Å. According to Makovicky *et al.* (2010), the $M(2)$ site could host Pb. In type material, there are 0.9 Pb apfu, whereas the specimen studied in this work is Pb-poor, with only 0.12 Pb apfu. Lead could be hosted at $M(2)$, however no evidence was found during the structure analysis. Indeed, bond-valence sums for $M(2a)$ and $M(2b)$ sub-sites are in reasonable agreement with expected values, i.e. 2.28 *vs* 2.10 vu and 0.32 *vs* 0.30 vu, respectively.

The $M(3)$ site is located on the margins of the PbS-like slab and it is a pure Bi position. As for $M(1)$, it shows a short $M(3)$–S(6) distance of 2.643 Å. Also in this case, the anion is located on the interslab surface. The observed distance can be compared with 2.628 Å given by Makovicky *et al.* (2010) for dantopaite. The $M(3)$ has two additional relatively short bonds (2.829 Å, longer than those reported by Makovicky *et al.*, 2010, i.e. 2.779 Å), two bonds at 2.983 Å and a long bond at 3.135 Å. The average <$M(3)$–S> distance is 2.900 Å, longer than that observed in the Austrian sample (2.857 Å – Makovicky *et al.*, 2010). As for the $M(1)$ site, $M(3)$ is also slightly overbonded,

https://doi.org/10.1180/mgm.2023.77 Published online by Cambridge University Press

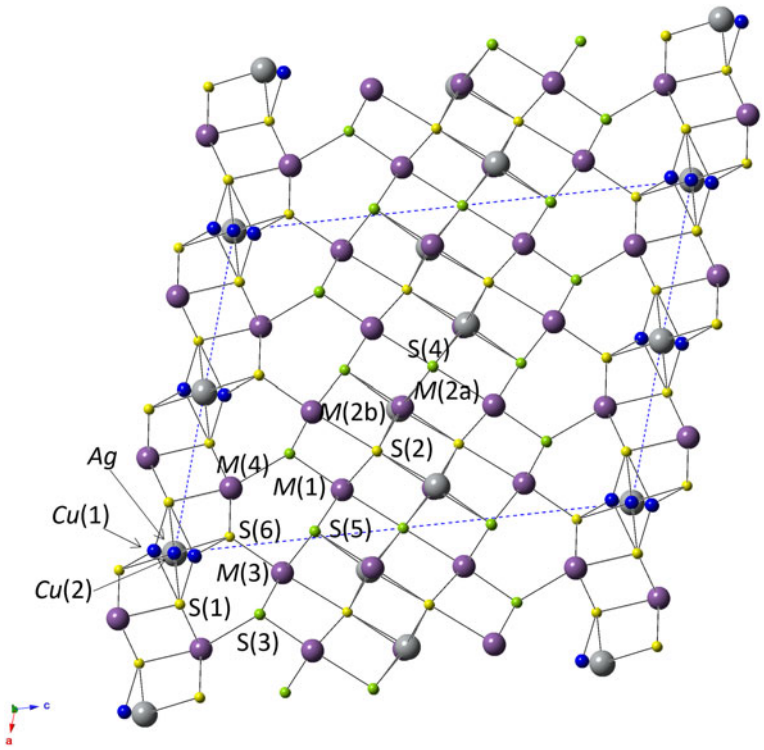

Figure 3. Crystal structure of Se-bearing dantopaite as seen down **b**. Violet, grey and blue circles represent Bi, Ag and Cu-hosting sites, whereas yellow and green circles show S- and Se-dominant positions. Drawn using *CrystalMaker*® software.

with a bond-valence sum of 2.81 vu, compared with a calculated value of 2.66 vu based on the Bi/Ag ratio.

The thinner slab contains single columns of edge-sharing Ag-centred octahedra (*Ag* site), flanked by double columns of Bi-centred square pyramids [*M*(4) site].

The *Ag* site has a 2+4 distorted octahedral coordination, with two linearly arranged *Ag*–S(6) bonds, with distance of 2.376 Å and a S(6)–*Ag*–S(6) angle of 180.0(2)°. Four additional bonds at 2.940 Å complete the bonding environment of this position. The site occupancy points to a partially occupied *Ag* position ($Ag_{0.66}$). Actually, the smaller *Ag*–S(6) distance observed with respect to that reported by Makovicky *et al.* (2010) (~2.50 Å) may suggest the partial replacement of Ag by Cu, in agreement with the overbonding of the bond-valence sum at the *Ag* site (Table 7). However, the average bond distance, 2.752 Å, is only slightly smaller than that in the corresponding Ag1 site of the sample from Erzwies, 2.764 Å. The shortest distances at the *Ag* site can be compared with those observed in linearly-coordinated Ag atoms in other minerals, e.g. ~2.45 Å in pyrargyrite (Laufek *et al.*, 2010), 2.432 Å in pyrostilpnite (Biagioni *et al.*, 2020) and 2.416 Å in neyite (Makovicky *et al.*, 2001).

In agreement with the structural model of dantopaite proposed by Makovicky *et al.* (2010), the *Ag*-centred octahedron is flanked by partially occupied, tetrahedrally coordinated, Cu-centred sites, namely *Cu*(1) and *Cu*(2). The *Cu*(1) site is situated along the column of Ag octahedra, between two adjacent polyhedra. Its average bond distance is 2.44 Å, to be compared with 2.41 Å observed by Makovicky *et al.* (2010). However, in Se-bearing dantopaite, the coordination tetrahedron is very distorted, with a very short distance of 2.09 Å and two long distances at 2.62 Å; on the contrary, the tetrahedron described by Makovicky *et al.* (2010) was more regular, with distances ranging between 2.35 and 2.50 Å. The *Cu*(2) site is located above and below the *Ag* site. Its average bond distance, 2.47 Å, can be compared with the value given by Makovicky *et al.* (2010), 2.54 Å. The *Cu*(1) and *Cu*(2) sites have occupancies $Cu_{0.10}$ and $Cu_{0.21}$, respectively; with respect to dantopaite from Erzwies, *Cu*(1) has a lower occupancy (0.10 *vs* 0.20), whereas *Cu*(2) is more occupied (0.21 *vs* 0.08). Considering site multiplicity, an excess of 0.57 apfu occurs, to be compared with the excess found during electron microprobe analysis (0.55 apfu). Such accumulation of Ag and Cu requires an ordering of these elements to avoid too short Me–Me contacts. Indeed, several short distances can be observed (in Å): *Cu*(1)–*Cu*(2) = 1.19(4), *Ag*–*Cu*(2) = 1.20(3), *Cu*(1)–*Cu*(1) = 1.69(11), *Cu*(2)–*Cu*(2) = 1.69(7), and *Ag*–*Cu*(1) = 2.21(2). An acceptable distance is represented by *Ag*–*Cu*(2) = 2.89(3) Å, whereas the distance *Cu*(2)–*Cu*(2) = 2.40(7) Å is shorter than the Cu–Cu distance in metallic Cu (e.g. 2.56 Å – Otte, 1961). However, as these sites show high values of their displacement parameters, it is possible that they may deviate from their average positions giving rise to tolerable bond lengths, favouring the occurrence of the metal excess observed in dantopaite.

The *M*(4) site has a square pyramidal coordination (average distance 2.825 Å), with two additional longer bonds at 3.479 Å. This site was refined as a pure Bi position; the occurrence of minor Pb cannot be excluded, as the bond-valence sum shows a small underbonding (2.87 vu), possibly agreeing with the presence of minor Pb. Usually, Pb replaces Bi in the thick slab (e.g. Makovicky *et al.*, 1977; Makovicky and Mumme, 1979), but Topa *et al.* (2008) described the occurrence of Pb in the thin slab of cupromakovickyite. However, this deviation from the expected value is probably within the experimental error and consequently the actual location of Pb in Se-bearing dantopaite cannot be found.

Among the six independent anion sites, three are dominated by S, i.e. S(1), S(2) and S(6), whereas the remaining sites have

https://doi.org/10.1180/mgm.2023.77 Published online by Cambridge University Press

Se > S. The bond-valence sums at these sites range between 2.02 and 2.16 vu, close to the expected value of 2 vu; only S (4) has a high value of 2.32 vu, indicating too short Me–anion bonds. As this position is bonded to the split site *M* (2) and shows the highest U_{eq} value among anion sites, it could be possible that the actual position of the atoms could be slightly displaced from the average position refined during this study.

The chemical formula obtained through single-crystal X-ray diffraction is $^{t}[Cu_{1.47}Ag_{1.32}Bi_4(S_{6.92}Se_{1.08})_{\Sigma 8.00}]$ $^{T}[Ag_{3.20}Bi_{8.79}(Se_{7.64}S_{6.36})_{\Sigma 14.00}]$, where superscript *t* and *T* indicate thin and thick slabs, respectively. It is worth noting that the *t* and *T* slabs have Se/(S+Se) ratios of 0.135 and 0.546, respectively, indicating the preferential partitioning of Se in the PbS-like thick slab, whereas the thin slab preferentially hosts S. The sum of these two *t* and *T* structural modules gives the formula $Cu_{1.24}Ag_{4.52}Bi_{12.79}(S_{13.28}Se_{8.72})_{\Sigma 22.00}$ ($Z = 1$) that can be compared with that obtained through quantitative chemical analysis, i.e. $Cu_{1.36}Ag_{4.39}Pb_{0.12}Bi_{12.62}Sb_{0.06}(S_{14.01}Se_{7.91}Te_{0.08})$. The number of electrons e^- refined at the cation positions is 1309.97, to be compared with 1306.13 e^- calculated from the chemical data. As regards the anions, 497.26 electrons expected on the basis of chemical data can be compared with 508.96 e^- obtained during the crystal structure refinement.

Nomenclature issues

Following the results of the crystal structure analysis, the 'substitution-free' formula of the sample studied in this work is $Ag_5Bi_{13}S_{12}Se_{10}$, being an intermediate member between dantopaite, $Ag_5Bi_{13}S_{22}$ (Makovicky *et al.*, 2010), and a hypothetical Se-end-member with formula $Ag_5Bi_{13}Se_{22}$. Following Nickel and Grice (1998), the sample of Se-bearing dantopaite could be theoretically considered as a different mineral species, because "*at least one structural site* [...]" is "*predominantly occupied by a different chemical component than that which occurs in the equivalent site in an existing mineral species*".

The occurrence of Se in pavonite homologues was previously known. Topa and Paar (2008), for instance, reported 0.25 Se apfu in cupromakovickyite, and up to 0.10 Se apfu were found by Žák *et al.* (1994) in makovickyite. Finally, Kolitsch *et al.* (2019) described the possible existence of the Se-analogue of dantopaite from the Clara mine, Germany. However, to the best of our knowledge, no structural data about the roles of Se in pavonite homologous series have been available so far. The study of Se-bearing dantopaite from the Mohawk mine shows a preferential partitioning of Se in the PbS-like slab, in agreement with the existence of the Se-isotype of galena, clausthalite. However, it is not clear what the maximum Se content in dantopaite isotypes could be; the rare grains showing higher Pb and Se contents than those measured in the structurally characterised grain suggest that further Se may be hosted in the PbS-like slab, probably increasing the Se/(Se+S) atomic ratio at the S(2)–S(5) sites. A full replacement of S by Se in this slab would lead to the chemical formula $Ag_5Bi_{13}Se_{14}S_8$. However if the Se-to-S replacement is assumed to also occur in the thin slab, the existence of $Ag_5Bi_{13}Se_{22}$ would be possible.

For the sake of simplicity, we think that S(1)–S(6) sites should be considered as an aggregate site for nomenclature purposes, avoiding the creation of different isotypes of dantopaite based on different S/Se ratios. On the contrary, species with S > Se should be classified as dantopaite, and those with Se > S could be described as a new mineral species.

Conclusion

The crystal chemical study of Te-rich stibiogoldfieldite and Se-bearing dantopaite allows the addition of new data, improving the knowledge of these very rare sulfosalt species.

The occurrence of vacancies at the *M*(2) site of stibiogoldfieldite related to the high Te content was confirmed, supporting the results of previous studies (e.g. Dmitrieva *et al.*, 1987; Pohl *et al.*, 1996). This new crystal structure refinement completes the first description of stibiogoldfieldite provided by Biagioni *et al.* (2022a), adding structural data for cotype material.

More interesting results have been achieved in the crystal chemical study of Se-bearing dantopaite. Indeed, this is the first investigation of a Se-rich natural member of the pavonite homologous series and its structural characterisation allows a description of the different S and Se partitioning between the two different structural slabs typical of this series. In particular, Se is preferentially hosted in the PbS-like slab, whereas S is located in the thin slab. This finding supports the possible natural occurrence of Se-dominant homologues of the pavonite series, confirming the results of Kolitsch *et al.* (2019) who suggested the occurrence of the Se-isotype of dantopaite at the Clara mine, Germany. Further research on the crystal chemistry of dantopaite and related phases will improve our understanding of the crystal chemistry of this complex homologous series of sulfosalts.

Acknowledgements. The paper was improved through the comments of the Associate Editor Owen Missen and two anonymous reviewers. CB acknowledges financial support from the Ministero dell'Istruzione, dell'Università e della Ricerca through the project PRIN 2017 "TEOREM – deciphering geological processes using Terrestrial and Extraterrestrial ORE Minerals", prot. 2017AK8C32. The Centro per l'Integrazione della Strumentazione scientifica dell'Università di Pisa (C.I.S.U.P.) is acknowledged for the access to the C.I.S.U.P. X-ray Laboratory. The study was also financially supported by the Ministry of Culture of the Czech Republic (long-term project DKRVO 2024–2028/1.II.a; National Museum, 00023272) for JS and ZD.

Supplementary material. The supplementary material for this article can be found at https://doi.org/10.1180/mgm.2023.77.

Competing interests. The authors declare none.

References

Biagioni C., Zaccarini F., Roth P. and Bindi L. (2020) Progress in the knowledge of 'ruby silvers': New structural and chemical data of pyrostilpnite, Ag_3SbS_3. *Mineralogical Magazine*, **84**, 463–467.

Biagioni C., Sejkora J., Musetti S., Makovicky E., Pagano R., Pasero M. and Dolníček Z. (2022a) Stibiogoldfieldite, $Cu_{12}(Sb_2Te_2)S_{13}$, a new tetrahedrite-group mineral. *Mineralogical Magazine*, **86**, 168–175.

Biagioni C., Sejkora J., Moëlo Y., Marcoux E., Mauro D. and Dolníček Z. (2022b) Tennantite-(Cu), $Cu_{12}As_4S_{13}$, from Layo, Arequipa Department, Peru: a new addition to the tetrahedrite-group minerals. *Mineralogical Magazine*, **86**, 331–339.

Brese N.E. and O'Keeffe M. (1991) Bond-valence parameters for solids. *Acta Crystallographica*, **B47**, 192–197

Dmitrieva M.T., Yefremov V.A. and Kovalenker V.A. (1987) Crystal structure of As-goldfieldite. *Doklady Akademii Nauk SSSR, Earth Science Section*, **297**, 141–144 [in Russian].

Flack H.D. (1983) On enantiomorph-polarity estimation. *Acta Crystallographica*, **A39**, 876–881.

Jeleň S., Pršek J., Kovalenker V.A., Topa D., Sejkora J., Števko M. and Ozdín D. (2012) Bismuth sulfosalts of the cuprobismutite, pavonite and aikinite series from the Rozália mine, Hodruša-Hámre, Slovakia. *The Canadian Mineralogist*, **50**, 325–340.

Johnson M.L. and Jeanloz R. (1983) A Brillouin-zone model for compositional variation in tetrahedrite. *American Mineralogist*, **68**, 220–226.

Kalbskopf R. (1974) Synthese und Kristallstruktur von $Cu_{12-x}Te_4S_{13}$, dem Tellur-Endglied der Fahlerze. *Tschermaks Mineralogische und Petrographische Mitteilungen*, **21**, 1–10.

Karup-Møller S. and Makovicky E. (1979) On pavonite, cupropavonite, benjaminite and «oversubstituted» gustavite. *Bulletin de Minéralogie*, **102**, 351–367.

Kolitsch U., Bayerl R. and Topa D. (2019) Neufunde aus der Grube Clara in mittleren Schwarzwald (V). *Mineralien-Welt*, **30**, 12–27.

Laufek F., Sejkora J. and Dušek M. (2010) The role of silver in the crystal structure of pyrargyrite: single crystal X-ray diffraction study. *Journal of Geosciences*, **55**, 161–167.

Makovicky E. and Mumme W.G. (1979) The crystal structure of benjaminite, $Cu_{0.5}Ag_{2.3}Pb_{0.4}Bi_{6.8}S_{12}$. *The Canadian Mineralogist*, **17**, 607–618.

Makovicky E., Mumme W.G. and Watts J.A. (1977) The crystal structure of synthetic pavonite, $AgBi_3S_5$, and the definition of the pavonite homologous series. *The Canadian Mineralogist*, **15**, 339–348.

Makovicky E., Balić-Žunić T. and Topa D. (2001) The crystal structure of neyite, $Ag_2Cu_6Pb_{25}Bi_{26}S_{68}$. *The Canadian Mineralogist*, **39**, 1365–1376.

Makovicky E., Paar W.H., Putz H. and Zagler G. (2010) Dantopaite, $Ag_5Bi_{13}S_{22}$, the ^{6}P natural member of the pavonite homologous series, from Erzwies, Austria. *The Canadian Mineralogist*, **48**, 467–481.

Nickel E.H. and Grice J.D. (1998) The IMA Commission on New Minerals and Mineral Names: procedures and guidelines on mineral nomenclature, 1998. *The Canadian Mineralogist*, **36**, 913–926.

Otte H.M. (1961) Lattice parameter determinations with an X-ray spectrogoniometer by the Debye-Scherrer method and the effect of specimen condition. *Journal of Applied Physics*, **32**, 1536–1546.

Pohl D., Ließmann W. and Okrugin V.M. (1996) Rietveld analysis of selenium-bearing goldfieldites. *Neues Jahrbuch für Mineralogie, Monatshefte*, **1996**, 1–8.

Pouchou J.L. and Pichoir F. (1985) "PAP" (φρZ) procedure for improved quantitative microanalysis. Pp. 104–106 in: *Microbeam Analysis* (J.T. Armstrong, editor). San Francisco Press, San Francisco.

Sejkora J., Biagioni C., Vrtiška L. and Moëlo Y. (2021) Zvěstovite-(Zn), $Ag_6(Ag_4Zn_2)As_4S_{13}$, a new tetrahedrite-group mineral from Zvěstov, Czech Republic. *Mineralogical Magazine*, **85**, 716–724.

Sheldrick G.M. (2015) Crystal Structure Refinement with SHELXL. *Acta Crystallographica*, **C71**, 3–8.

Shimizu M. and Stanley C.J. (1991) Coupled substitution in goldfieldite–tetrahedrite minerals from the Iriki mine, Japan. *Mineralogical Magazine*, **55**, 515–519.

Topa D. and Paar W.H. (2008) Cupromakovickyite, $Cu_8Pb_4Ag_2Bi_{18}S_{36}$, a new mineral species of the pavonite homologous series. *The Canadian Mineralogist*, **46**, 503–514.

Topa D., Makovicky E. and Balić-Žunić T. (2008) What is the reason for the doubled unit-cell volumes of copper-lead-rich pavonite homologues? The crystal structures of cupromakovickyite and makovickyite. *The Canadian Mineralogist*, **46**, 515–523.

Welch M.D., Stanley C.J., Spratt J. and Mills S.J. (2018) Rozhdestvenskayaite $Ag_{10}Zn_2Sb_4S_{13}$ and argentotetrahedrite $Ag_6Cu_4(Fe^{2+},Zn)_2Sb_4S_{13}$: two Ag-dominant members of the tetrahedrite group. *European Journal of Mineralogy*, **30**, 1163–1172.

Wilson A.J.C. (1992) *International Tables for Crystallography. Volume C*. Kluwer, Dordrecht, The Netherlands.

Žák L., Frýda J., Mumme W.G. and Paar W.H. (1994) Makovickyite, $Ag_{1.5}Bi_{5.5}S_9$, from Baita Bihorului, Romania: The ^{4}P natural mineral member of the pavonite series. *Neues Jahrbuch für Mineralogie, Abhandlungen*, **168**, 147–169.

https://doi.org/10.1180/mgm.2023.77 Published online by Cambridge University Press